Laser Processes for Prototyping and Production of Novel Microfluidic Structures

John R. Andrews and Bradley Gerner
Xerox Wilson Center for Research and Technology
800 Phillips Rd. MS/114-44D
Webster, NY 14580
Email: jandrews@crt.xerox.com

ABSTRACT

We describe a number of microfluidic components that have been formed by laser micromachining and incorporated in a picoliter droplet dispenser. The laser micromachined structures include an adhesive interface between macrofluidic and microfluidic regions, a particle filter, a fluid manifold, channels, and nozzles. Both excimer laser and CO_2 laser processes are used.

Keywords: microfluidics, filter, nozzle, channel, ink jet, excimer laser, CO_2 laser, manufacturing, MEMS, wafer-scale assembly

1. INTRODUCTION

Microfluidic devices require a range of functionality to complete complex tasks. Flexibility in the selection of materials is also useful to insure compatibility with other aspects of a particular application. For the development of microfluidic structures the ability to quickly prototype devices is critical. If these devices are to be economically important, they must be brought to market using cost effective production methods. Laser micromachining offers opportunities in each of these aspects of microfluidic technology. In this talk we will describe a number of microfluidic devices fabricated using laser micromachining. These devices include fluid interconnects, filters, nozzles, complex fluid pathways, on-wafer processing and fully assembled microfluidic systems. Some of these laser micromachined devices have gone to production in the millions of parts per year and others would lend themselves to volume production by laser micromachining. Some considerations in extending laser micromachining from prototyping to production of microfluidic components and devices will be described.

The quintessential microfluidic device is found in ink jet printers[1]. Explosive boiling is used in thermal ink jet, wall shear-mode piezoelectric transducers, bilayer expansion mode piezoelectric transducers, and thermomechanical are the primary fluid pumping mechanisms. Of growing economic importance are medical assay devices for clinical and consumer use. Additionally, advanced concepts such as the chemistry lab on a chip will drive additional developments in microfluidic capability. Many microfluidic devices require a suite of different passive functional components to develop a fully functional unit.

A suite of microfluidic device structures for practical microfluidic devices includes: 1) Interface between the macroscopic and microscopic fluid structures, 2) Particle filters that prevent clogging of the microfluidic pathways, 3) Channels and chambers to permit routing and mixing of fluids from different sources, and 4) Nozzles for dispensing the fluids. A significant cost reducing strategy for microfluidic devices is to process these devices on a wafer scale so that a large quantity of multilayer devices can be produced in a single assembly step.

There are a range of microfluidic device structures. Polymers[2] provide the most widely used material for microfluidic structures, but a wide range of other materials can be used. In this talk we will describe how laser micromachining is

Microfluidics, BioMEMS, and Medical Microsystems II, edited
by Peter Woias, Ian Papautsky, Proceedings of SPIE Vol. 5345
(SPIE, Bellingham, WA, 2004) · 0277-786X/04/$15 · doi: 10.1117/12.524547

used to make a number of different structures that have utility for different fluid paths. The use of a CO_2 laser provides high throughput and low cost structures for intermediate resolution geometries in the 100 μm-size and larger. It is particularly effective for patterning film adhesives with feature sizes that are smaller and at higher density than can easily be done by die cutting. For smaller features and especially for polyimide, the KrF excimer laser at 248 nm provides an especially effective micromachining tool[3-5]. Further, if the structures being created are at high density, then the imaging mode of excimer laser micromachining can make effective use of the large pulse energies available from excimer lasers by spreading it over a large area.

In the following sections we will outline the microfluidic structures that were developed and create key microfluidic pathways using various materials and laser micromachining. Some of these structures are efficiently used for high volume production of the various structures. Other features described will be most interesting in rapid prototyping or small volume production.

2. LIQUID DROPLET DISPENSER

The liquid "droplet dispenser" in this discussion is an edge-shooter thermal ink jet printhead. It is not the purpose of this paper to discuss in detail the design and fabrication of thermal ink jet printheads, but to use the thermal ink jet printhead as a "microfluidic" breadboard in which a number of laser micromachined features are included.

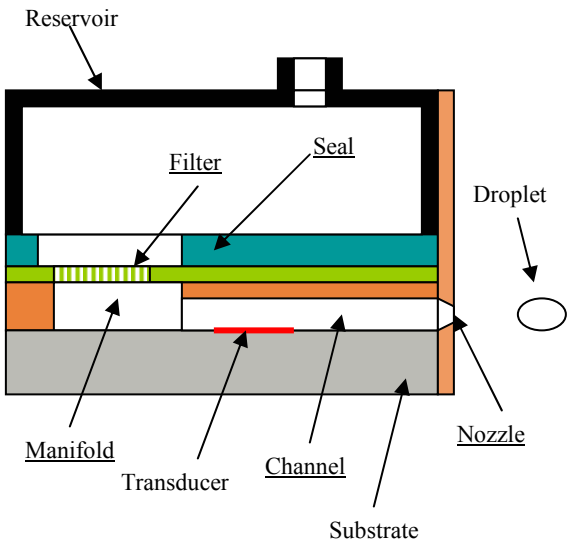

Fig. 1. A cross-sectional view of a picoliter drop dispenser based upon the basic design geometry a thermal ink jet printhead. The microfluidic elements described below have underlined labels.

A cross-sectional view of the microfluidic structure is shown in Fig. 1. Along the axis running into the page, there is an array of channels and nozzles attached to a common manifold. Liquid enters the reservoir through a port at the top. The reservoir is part of the macroscopic world being several millimeters in dimension. The reservoir is attached to the basic microfluidic structure by an adhesive element. The attachment of the reservoir to the microfluidic dispenser has several requirements. The attachment needs to provide a good fluid seal. It needs to accurately match features on both the macroscopic side and microscopic side of the attachment. It cannot shed particles that will create blockage downstream. It needs to be chemically compatible with the liquid and and it's additives. The second element is a particle filter. The filter is important in preventing macroscopic particles (i.e., any particle larger than the smallest microfluidic passage) from entering the microfluidic device. The microfluidic passage includes a manifold feeding an array of channels. In an ink jet applications there might be 3 or 4 separate manifolds to accommodate the three primary colors and black. The manifold is attached to an array of channels, each of which contains a pressure-generating element. The pressure-generating transducer is a heater in thermal ink jet, where the heater superheats water to the point of explosive boiling. The pressure generating transducer need not be a heater however. Finally, the channel is terminated in a nozzle. The nozzle is typically much smaller than the channel and must be precisely aligned to it.

3. FLUID SEAL

The fluid seal is made from a double-sided tape. A cross-sectional view of the tape is shown in Fig. 2. The tape as delivered is 5 layers. The top layer is a release liner and the bottom layer is a carrier. Both of these are made from polyester. The functional tape consists of a polyester substrate with an adhesive layer on either side. The materials come in a roll and the tape is fed into the laser cutting zone with a reel-to-reel feed system. In different applications phenolic nitrile or epoxy adhesives have been used. A photograph of a finished fluid seal is shown in Fig. 3. The tape

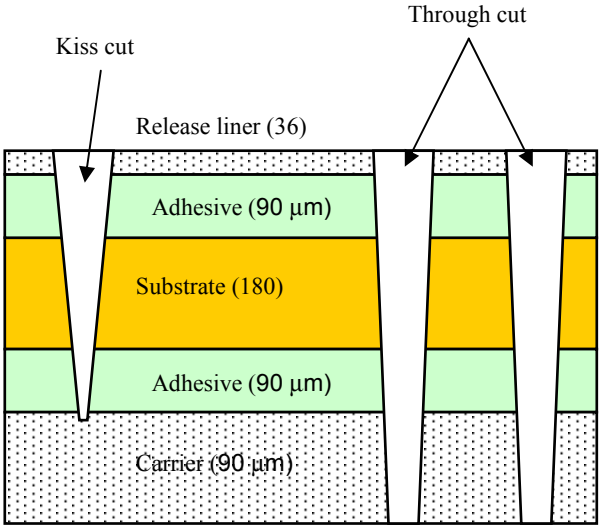

Fig. 2. A cross-sectional view of the double-sided tape used to attach the fluid reservoir to the macroscopic side of the microfluidic structure. The release liner, substrate, and carrier are polyester films. The adhesive was either phenolic nitrile and epoxy adhesives

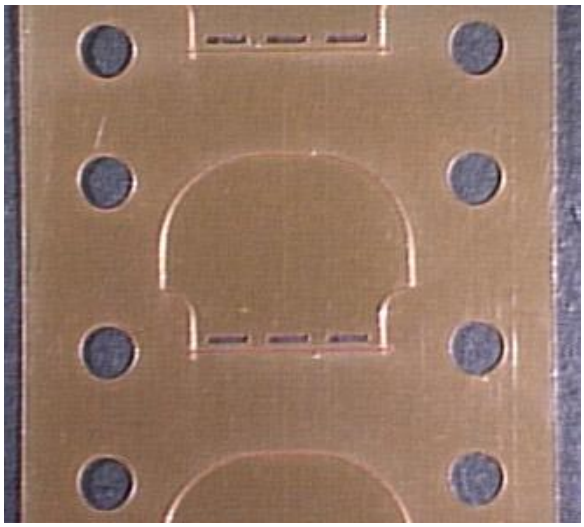

Fig. 3. A picture of a completed fluid seal that is cut from a continuous tape. The three elliptical fluid feed-throughs have the slugs removed as are the slugs from the round sprocket holes.

is 40 mm wide. In the center of the photograph is one complete part. Portions of the preceding part and subsequent part are shown in the top and bottom of the photograph. The 4 mm diameter holes running down either side of the tape are sprocket holes. In the laser cutting tool, the tape is advanced with pneumatic clamps. The sprocket holes are used in the part delivery system in the automated assembly tool. The part itself consists of through cuts for the 3 fluid pass-throughs and the part perimeter is a kiss-cut. The differences in these cuts are illustrated in Fig. 2. The through cut is a trepan of the 3 mm X 0.5 mm slot. Vacuum behind the part extracts the slug during cutting. The kiss-cut defines the perimeter of the part. For the kiss cut, the cut depth is critical since the part needs to remain solidly within the strip, but the adhesive must be completely severed to insure clean removal of the part on the assembly line. Perturbation of the uncut base adhesive during the picking of the part could also permit leaks in the assembled part. Although the part and features are relatively large, the tolerances for the part are quite tight. The slot size and location tolerances are both 0.05 mm. To retain the strength of the carrier, the cut depth for the kiss-cut tolerance was ±0.025 mm from the center of the carrier.

Die cutting would be an option to explore for creating a part such as this. However, die cutting could not achieve several objectives for this part. A clean fluid feed-through was not obtained. Figure 4 shows a die cut slot (A) and a laser cut slot (B) with the top release liner removed exposing the adhesive. The die cut slot is rough and has adhesive strands separated from the film. Frequently, polyester strands were also observed. These irregularities prevented achievement of the position and size tolerances. The fibers generated during die

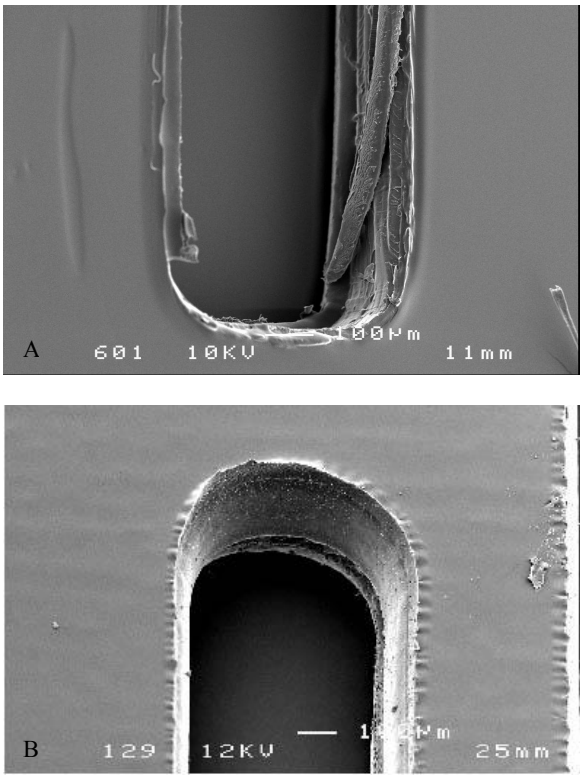

Fig. 4. A close-up of the fluid feed-through for A) a die cut part and B) the laser cut part that was made in production.

cutting would some times fold over and create a leak pathway between the slots or to the external world. In contrast, the laser cut edge can be seen in Fig. 4 (B). The extremely smooth edge is in sharp contrast to the die cut slot. The small heat-affected zone (HAZ) of ~50 μm is also very narrow and reproducible.

A number of laser cutting methods were evaluated for making this fluid seal, including both RF discharge and TEA CO_2 lasers at both 10.6 μm and 9.4 μm, KrF excimer laser at 248 nm, and the 3rd harmonic of the diode pumped Nd:YAG laser at 355 nm. The excimer laser cutting, not surprisingly, was relatively slow and when cutting at maximum rate had a significant HAZ. The TEA CO_2 laser used in imaging mode for area ablation had HAZ and under aggressive machining conditions left carbonized material at the cut edge. The Nd:YAG 3rd harmonic was very slow cutting and still resulted in some HAZ. The RF discharge CO_2 laser provided fast cutting. At 10.6 μm, the HAZ was ~2X larger than for the 9.4 μm laser under similarly optimized cutting conditions. The rational for this difference was evident in the infrared absorption spectra of both polyester and the adhesives. There were significant absorption bands in the 9.4 μm spectral region for all of these materials that were absent from the longer wavelength. Thus, the optical coupling to the tape was higher, thus intensifying and localizing the heating effects that lead to cutting by material removal.

The production system was a 9.4 μm CO_2 laser scanned by a dual-axis galvanometer through a telecentric scan lens having a numerical aperture of ~0.1 and a focused spot size of ~80 μm. The slowest scan speed used in making the part was 250 mm/s for cutting the slots at a peak power of ~20W. A reel-to-reel tape transport system indexed tape through the cutting zone. The substrate holder under the cutting zone supplied vacuum hold down and slug extraction. The system included closed loop feedback to control to stabilize the laser power. The power set point was adjusted based upon an inline measurement of the material thickness. The set point adjustment insured that the kiss cut depth did not get too shallow and leave some adhesive intact across the part edge and also insured that the depth of the cut was not so deep as to weaken the attachment of the part to the tape. The high speed cutting and substantial material vaporization required an enclosed exhaust extraction system. An inline inspection system measured all of the key features and issued a pass/fail based upon pre-set criteria. An ink marker system identified any failed parts in a way that the automated assembly system could recognize and skip the failed parts. The only significant failure mechanism was un-extracted slugs for which a failure rate of <0.5% was seen.

		SLOT 1				SLOT 2				SLOT 3			
		X	Y	Width	Height	X	Y	Width	Height	X	Y	Width	Height
	Target	3,075	890	3,035	440	7,580	890	3,035	440	12,145	890	3,035	440
Run	Count												
C1	1979	3,072	879	3,034	449	7,575	898	3,031	424	12,142	898	3,044	429
C2	2511	3,074	884	3,035	457	7,579	902	3,028	433	12,142	899	3,049	441
C3	1859	3,071	884	3,024	454	7,581	903	3,026		12,146	895	3,039	447
C4	2502	3,070	884	3,024	455	7,578	903	3,025	434	12,139	896	3,042	442
Std. Dev.		13	7	22	16	12	8	21	14	17	9	30	17

Table 1. The average location (X, Y) and dimensions (Width, Height) of the 3 slots in the fluid seal. Each production run (C1-C4) included approximately 2000 parts (Count). The standard deviation is cumulative for all of the parts in the four runs. Measurements were made with the inline measuring tools on the production system. All dimensions are in micrometers.

A summary of the performance of the system is shown in Table 1. The size and location of the slots through which the fluid moves from the manifold to the microfluidic device were critical to the system performance. Four runs are recorded here that include more than 8000 parts, each of which was measured by the inline inspection system. The average dimensions for the locations and sizes of slots for each run are shown. These locations can be compared to the target values shown at the top of the table. Two observations are critical to understanding the production performance of the system. First, the run-to-run variations in the dimensions are very small. Second, the standard deviations over a large number of parts is quite small, the largest being 30 μm with a more typical value being about 15 μm. Off-line

metrology, where defects in the liners can be eliminated, the typical standard deviation was about half of those measured in-line.

4. MICRO-PORE FILTER

A microfluidic system that receives liquids from an unprotected environment is sensitive to failure due to blockage of a channel by particles entering from the environment. Millipore and ceramic or metal frit filters can be very effective at removing even small particles, but the pressure drop across such a filter can be quite large. Woven or random mesh filters can have substantially lower pressure drop (<<1" H_2O). The mesh filters have a relatively high particle retention capacity but even a small leakage rate can create failures in a device that is sensitive to even a single particle over a certain size. One way to augment a high capacity mesh filter and insure that no element in a multi-channel array is blocked is to add a micro filter such as the one shown in Fig. 5. This picture shows a close-packed hexagonal array of holes etched in polyimide using a KrF excimer laser at 248 nm. This filter was installed in a working inkjet printhead (as shown schematically in Fig. 1) downstream from a 12 μm Absolute woven steel mesh filter. Analysis after several days of operation showed a number of particles trapped by these 12 μm laser-machined micro-filters. One such trapped particle is shown in the center of the electron micrograph. Inclusion of the filter was found to nearly eliminate the development of blocked channels over long-term operation. One advantage of the excimer machined filter is that it can be made in any pore size from ~2μm and larger. Most important for the ink jet printheads was the filter range of 10μm to 25μm. The filters can be made with a pore distribution of 1μm with any average size. The filter was optimized to the maximum size that would still insure no particles could block a channel so as to minimize flow resistance through the filter.

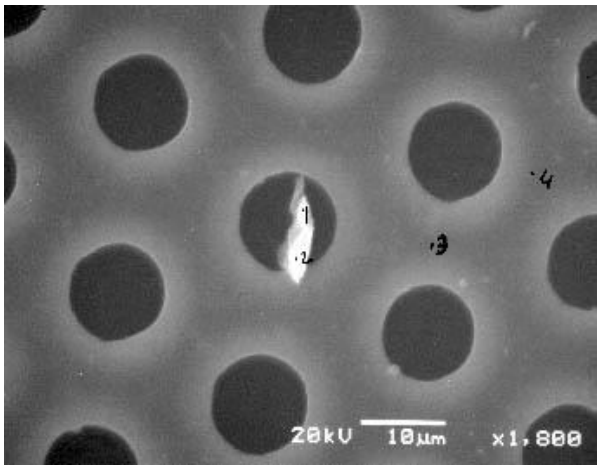

Fig.5. A scanning electron micrograph of a particle filter. This filter was evaluated after use. A trapped particle is shown trapped in one of the filter pores in the center of the micrograph.

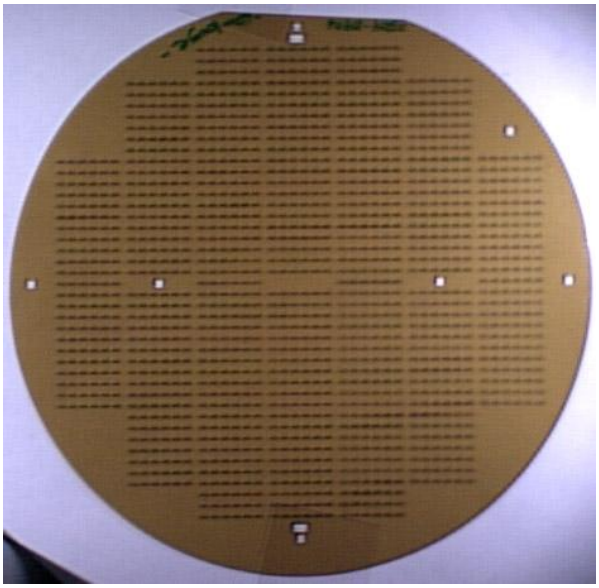

Fig 6. A photo micrograph of a film containing filters for over 350 fluidic devices made on a silicon hybrid micro fluidic/microelectronic wafer. The microfluidic devices are arranged in 7 columns. The film is bonded to the wafer in a single step.

The filters provide an excellent application for efficient use of an excimer laser in a production environment. In this case, over 350 microfluidic devices were created on a disk the size of a 5-inch silicon wafer. The polyimide film had been laser micromachined to have a filter to cover each of the fluid openings on the wafer. A picture of a filter disk is shown in Fig. 6. The filters for an individual microfluidic device consist of six rectangular elements placed in a line. The devices are arranged in 7 columns and 43 rows. The larger rectangular openings are windows through which alignment targets on the wafer could be seen. The filters were aligned to the silicon wafer and bonded while the wafers were still in the clean room and prior to dicing individual die out of the wafer. In this way, the microfluidic devices left the clean room only after they were protected from any

particles that were large enough to block any of the on-chip fluid pathways. As a result, no yield loss occurred due particle contamination in the dicing and packaging operations.

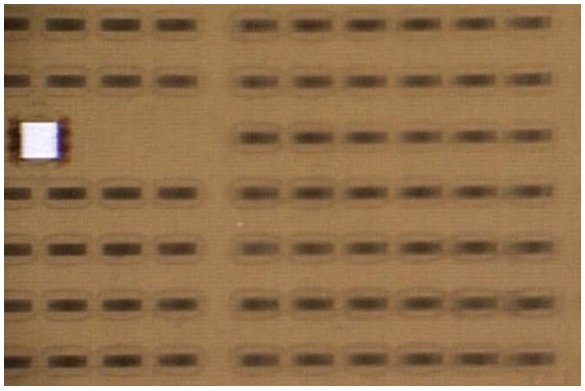

Fig.7. A close-up view of a piece of the filter array that appears in Fig. 6. The square is a window to expose an alignment target for wafer dicing. The filter for each device consists of 6 segments.

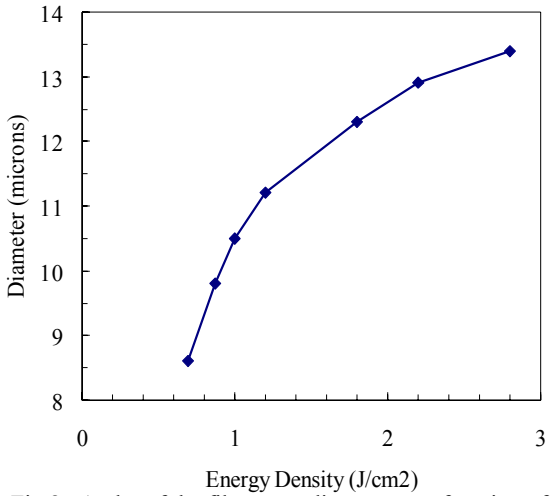

Fig.8. A plot of the filter pore diameter as a function of the laser energy density at the 25µm polyimide film for a projected image at the substrate of 15 µm in diameter

A close-up of a piece of the filter disk is shown in Fig. 7. One of the columns is on the right side of the picture, showing clearly the 6 elements in one column. The partial column on the left shows the window for the alignment target. Close observation shows a little residual laser ablation debris around each filter element. Plasma cleaning prior to adhesive bonding removed this debris around each filter element.

In addition to the particle retention distribution, a key parameter to evaluate the performance of a filter is the resistance it provides when inserted in the flow path. A filter of this type with 11µm pore size having an area of 0.88 mm^2, a flow rate through the filter of 10 µl/s with a fluid viscosity of 3.5 cp, has a pressure drop of 500 Pa (2 inches of H_2O).

There is much flexibility in the selection of the material for making the filters using excimer laser ablation. The selection of a filter substrate material is driven more by the specific requirements of the application. For this particular application, 25 µm polyimide was advantageous. A KrF excimer laser operating at 248 nm was the light source. A high aspect ratio beam homogenizer provided uniform illumination of a projection mask. A 5X, 0.1NA projection imaging system placed the reduced image of the chrome-on-quartz mask on the polyimide substrate. The 6 filter elements for a single device filled an area of 13.5 mm X 0.3 mm and were created in a single ablation operation. The entire filter disk was generated by step-and-repeat. The windows were created by laser ablation from a second mask element and motion of the second substrate stage. Figure 8 shows the relationship between the filter pore size and the energy density for a given filter mask. Operating at ~1 J/cm2, 50-75 pulses would be used to create the filter. For a 300 Hz excimer, each device filter array would take ~0.25 seconds to create. Using simple feedback control to maintain constant laser power it was possible to maintain a tolerance of 1 µm in the filter pore size. Long term drift was minimized by off-line measurements to provide feedback to make small adjustments in the energy density delivered to the substrate.

5. CHANNELS

Channels in a microfluidic system can route the fluid from one region to another. One means of creating channels on wafers is to spin on a photopolymer such as photoresist, polyimide, or SU-8. Though these photo-patterned and developed materials can be very convenient, there are a number of situations in which this is not an option. If the substrate is sensitive to the liquid for spin-on or development of the resist, this can be a problem. The liquids in the application can have a chemical interaction with the resists, precluding their use. A specific material may be needed in the application due to its chemical or physical properties. In some cases, the latitude for exposure and development of the resist materials might prevent creation of the entire range of features needed. For these situations, laser micromachining can be an attractive option for creating the microfluidic pathways. Early in the development of the

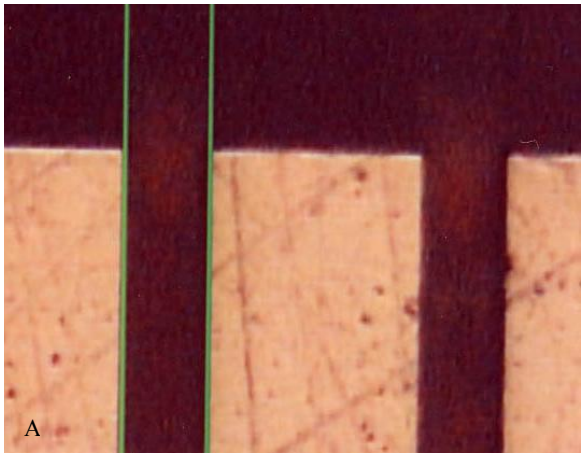

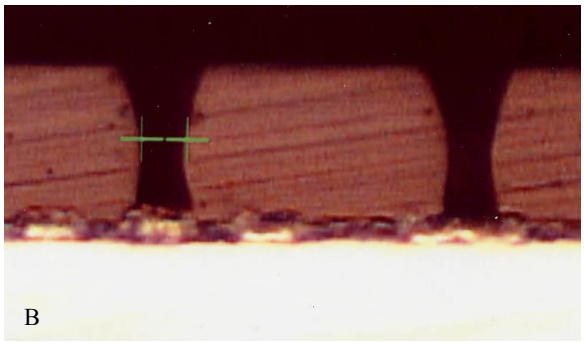

Fig.8. Laser cut channels in polyimide that has been spun-coated on a silicon microelectronic wafer. A) A view of two channels oriented in the vertical direction and a horizontal edge that was created by dicing the wafer after laser processing. B) The diced face of the channels that were formed by laser micromachining. The metallization on the wafer can be seen at the bottom of the channels.

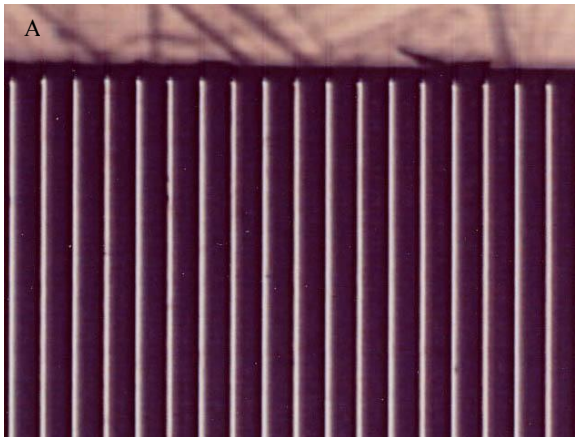

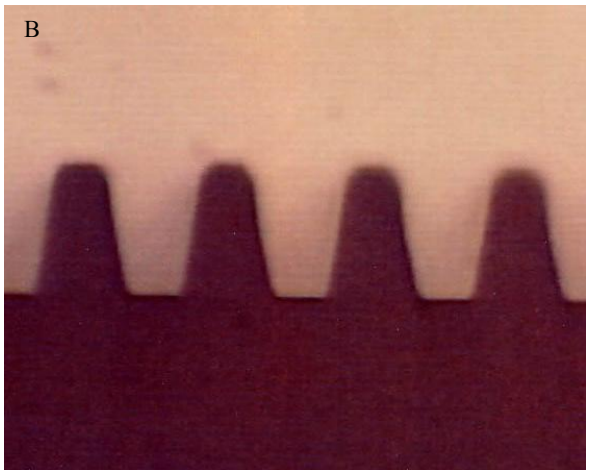

Fig.9. Two views of laser cut channels in a free-standing film of polyimide. A) A top view of the land areas from the top surface of the film. The dark edge at the top is the laser cut end of the channels. B) The end view of the laser cut channels from the manifold at higher magnification.

critical design parameters for a particular device, it might be useful to quickly prototype a wide range of fluid structures to test different design parameters. For ink jet and many other microfluidic applications, polymers provide a very convenient material to define the fluid pathways. For small features on the order of 2 μm to100 μm, excimer laser micromachining can prove advantageous.

An example of excimer laser micromachining of a polyimide spun on to a silicon wafer containing microelectronics and transducers is shown in Fig. 8. Channels are etched in a ~15 μm thick fully cured polyimide film. On the top surface (A) the channels are 8 μm wide. A cross-section created by dicing the wafer shows an hourglass shape. The narrow part of the channel is ~5 μm. The widening of the channels near the substrate is the result of reflection of the laser light off the substrate etching preferably near the substrate. The width at the bottom of the channel can be controlled by the energy density employed to do the etching and by the number of pulses in excess of etch-through that are used. The polymers cured in place on the wafer tend to etch quickly and at low energy density. This channel was etched with 15 pulses at 350 mJ/cm^2 using a KrF excimer laser operating at a wavelength of 248 nm. Rectangular mask openings were imaged to 8 μm at the substrate surface. Under these conditions it was possible to completely remove any polyimide on metal, dielectric or bare silicon without damage to the underlying layer.

Another example of laser-etched channels in a free-standing polyimide film is shown in Fig. 9. In (A) the array of channels is on a pitch of 42.3 μm and a small unperturbed area remains between each etched channel. At the top of (A)

one can see that the film has been etched completely through. Referring to Fig. 1, this etched through region would constitute the manifold where liquids feed the individual channels. The cross-section of the channels is shown in (B). Note the sloped walls and rounded top to the channel. This shape is a direct result of the formation process. An array of circular holes was imaged onto the substrate and the substrate translated during the firing of the laser. If the channels were made under identical conditions using a square or rectangular ablation illumination, the sidewalls would have a much smaller taper and a top that would appear nearly flat in cross-section.

The scanning method for creating channels is relatively slow. However, is provides the opportunity for great flexibility in the shape and size of the channels, the routing and connectivity can also be changed at will. Once the microfluidic design is complete, it is possible to transfer the design to a mask to permit image transfer ablation, making more efficient use of the excimer laser light.

6. MONOLITIHICALLY INTEGRATED MICROFLUIDICS

Though laser micromachining can be used to create a number of individual microfluidic functions as described above, these devices can have multiple integrated functions. The completed component can be laser micromachined in its entirety or an integration of multiple formation methods. One example of a hybrid formation method is shown in Fig. 10. This image shows nozzles that are etched through a wall of polyimide to connect with blind channels. The polyimide layer was spin-coated on a silicon microelectronic layer, patterned through conventional photolithography to provide fluid pathways including the blind channels. A second silicon wafer is placed over the polyimide to form the top for the fluid pathways, creating enclosed channels and an entry for the fluid. Dicing is used to create individual devices. The blind channels were then opened using laser ablation. The laser ablation method of opening the blind channels could have several advantages, depending on the specifics of the application. First, the nozzles can be round and symmetric openings for the photo lithographically formed rectangular channels. Second, opening the blind channels after dicing eliminates the potential contamination of the interior microfluidic surfaces with the fluids used to facilitate the dicing operation. For ink jet and possibly other application, it is convenient to coat the exit face of the microfluidic device with a hydrophobic coating. Placing that coating on a surface where the fluidic interior is not exposed and subsequently opening the blind channels insures that the coating does not contaminate the interior of the microfluidic device. As discussed above, the ablation of the photo lithographically patterned polyimides can be done at very low energy density (<500 mJ/cm^2).

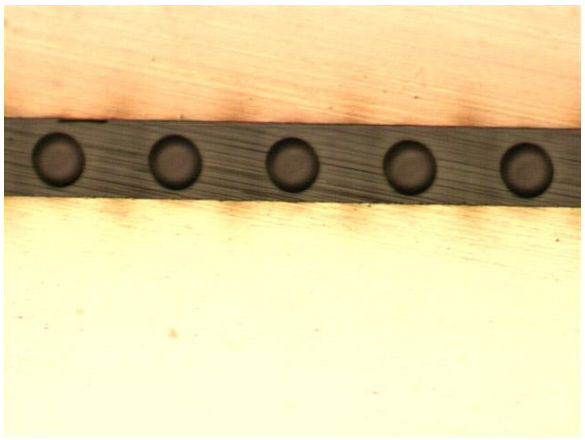

Fig. 10. Nozzles formed in the polymer layer between two silicon wafers. The nozzles are the exit to blind channels formed by photo patterning of channels. The face shown is formed by dicing the wafer pair.

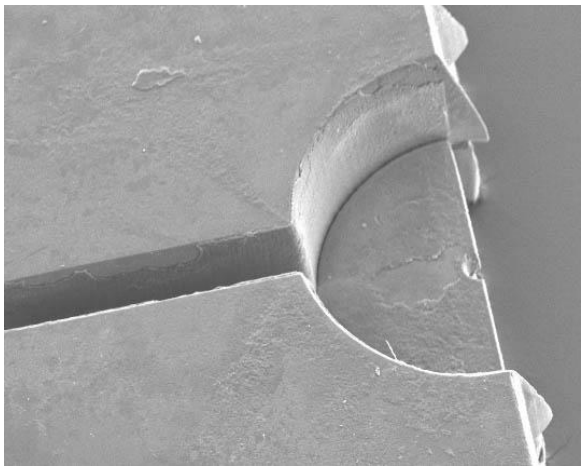

Fig. 11. A 4-layer etch process and 2-axis scanning is used to form the channel, chamber, recess, and nozzle.

A second example of integrated microfluidic functions is shown in Fig. 11. Here the laser micromachining is done in a free-standing polymer film (polyimide). In the figure one sees on the left a channel entering a fluid chamber, half of which remains in this cross-sectioned part. The channel is

etched to a depth that provides the appropriate flow characteristics for this particular application which entails tailoring both the flow resistance and inertance. The round chamber (1 mm in diameter) is etched partially through the film to a second depth, leaving a large circular chamber. This chamber is designed to contain an electromechanical pressure transducer. However, similar geometries could be used to combine reagents in a chemical or biochemical reaction. In the center of the cleaved edge of the chamber, there is a third etch level having a relatively small diameter. Inside the third etch level is a nozzle that forms a pathway to the outside of the microfluidic device. The third etch level is in place to provide a rigid wall for the large chamber and a low fluid resistance to the nozzle. The final microfluidic device is formed by bonding of the laser micromachined structure to a plate containing the electromechanical actuator.

7. NOZZLES

Nozzles may be the most critical part of any drop ejecting device. The volume of ejected liquid will typically be linearly proportional to the area of the nozzle over a significant range of area changes. The direction that the liquid droplet is ejected is critically dependent on the smoothness and symmetry of the nozzle. A scanning electron micrograph of two nozzles that are 20 µm in diameter and separated by 42.3 µm is shown in Fig. 10. The substrate is 25 µm polyimide. The roundness and absence of defects on the edges enables laser micromachining to be used for the wide scale production of inkjet nozzles. Figure 11 shows the cross section of one of these nozzles. Note the smooth roundness of the laser beam entrance side located on the top of the image. The low taper is especially important when packing nozzles at densities as high as 600 per inch. The nozzle in Fig. 1 is shown as part of a nozzle plate that is

Fig.10. Laser-ablated nozzles in polyimide.

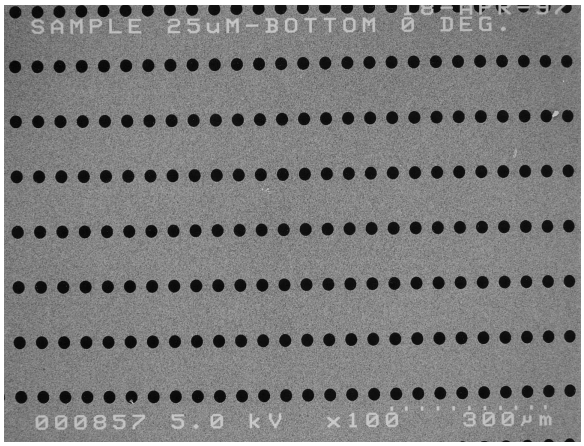

Fig.12. Multiple rows of nozzle arrays

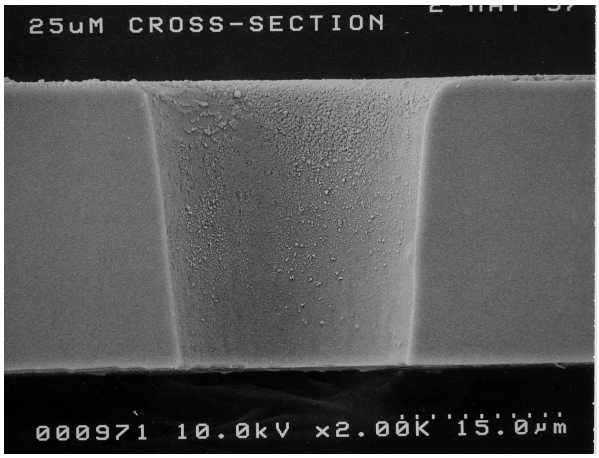

Fig.11. A cross-section of one nozzle formed in a 25 µm thick polyimide film.

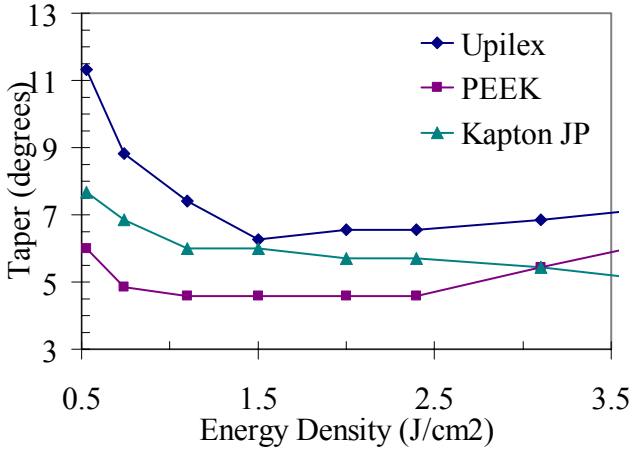

Fig.13. The cone half-angle of taper for three different 50 micron-thick films.

adhesively attached to an array of channels. A flat, unperturbed laser entrance surface on the nozzle plate is important to be able to form a leak-free seal between nozzles that is robust to fluid penetration. Figure 12 shows pieces of several arrays used to evaluate the consistency of the nozzle size and shape. The taper of the nozzle is shown in Fig. 13 for three different 50 μm thick freestanding films. The films are Upilex S polyimide, polyetheretherketone (PEEK), and Kapton JP polyimide. The nozzle taper at low energy density is different for each of these materials. In each case the taper decreases as the energy density increases. However, by ~1.5 J/cm2 the taper is near the minimum for each material. At higher energy densities, the taper starts to increase once again. The decrease in taper with higher energy density appears to be a result of the interaction of the laser light with the sidewalls of the hole where the high energy partially overcomes the efficient reflection from the steep sidewalls. The slow increase in taper at higher energy densities is the result of having the entrance hole size increasing at a rate that is higher than the increase of the hole on the exit side.

8. INTEGRATED MICROFLUIDIC AND MICROELECTRONIC DEVICE

The integration of laser micromachined microfluidics with silicon microelectronics is a feature of some commercial thermal ink jet printheads. An example of a high level of laser micromachined microfluidic components is shown in Fig. 15. The perspective is looking down on the structure shown in Fig. 1 but with the reservoir and top filter layer removed. In this picture a 15 mm long silicon die is shown having the microfluidic structures defined in transparent polyester films. A cross-section in a plane perpendicular to the paper and running vertically is shown in Fig. 16. At the top of the picture, the rectangles are bond pads for connecting the microelectronics on the silicon die to external

Fig. 15. A complete silicon microfluidic drop ejector containing 3 isolated fluid chambers. The cross-section is similar to that shown in Fig. 1 except the reservoir is not in place. The rectangles on the top edge are electrical contact pads fluid is ejected at the bottom edge.

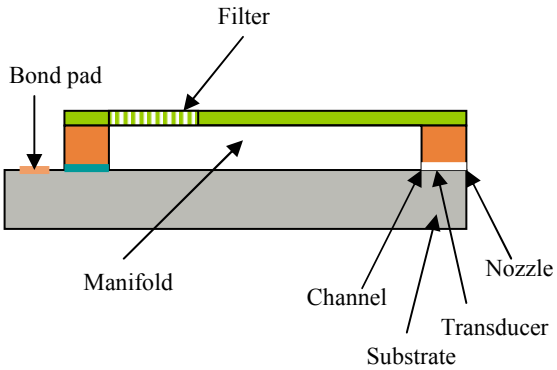

Fig. 16. A cross-section of the die shown in Fig. 15. The view is along a vertical plane perpendicular to the plane of the page.

electronics. The metallization associated with the microelectronics covers much of the rest of the die, except at the perimeter. The outlines of three trapezoidal regions are visible with the narrow part at the top and the wide bases nearly touching at the bottom edge of the die. The three trapezoids define 3 separate fluid paths. The micro-pore filters usually forming the top layer would be located along the top edge of the trapezoid. The fluid flows through the manifold and feeds in parallel approximately 100 channels, each of which contains a heater/transducer. Droplets are ejected along the bottom edge traveling in the plane of the page. Referring again to Fig. 16, the silicon wafer is labeled as the substrate. On top of the wafer is a 15 μm thick photo lithographically patterned polyimide that is removed in the manifold region. On the right hand side, the cross-section is taken through the center of the photo-lithographically defined channel in the polyimide. The second layer above the substrate is 125 μm thick polyester. Its bottom surface creates the top of the exit channels on the right and confines the fluid laterally elsewhere. The open volume forms the manifold through which fluids can flow with low resistance. The cover layer (not present in the photograph) is a 50 μm layer of polyester that seals the fluid chamber except in the location of the filter.

The two laser micromachined layers were both formed using excimer laser ablation. Both layers were formed in a wafer arrangement similar to that shown in Fig. 6. Each layer was aligned to the silicon substrate and bonded using thin adhesive layers. The filter was formed in a manner essentially identical to those formed in polyimide except that the energy density used was slightly lower. The large trapezoidal openings were formed using dual axis excimer laser ablation. In the dual axis scanning method, the mask is illuminated with a stationary beam. The mask and substrate are scanned in opposite directions due to the image inversion by the imaging lens. For the 5X demagnification between the mask and substrate, the mask is scanned at a velocity 5 times faster than the substrate. The dual axis scanning method permits transfer of ablation patterns that are larger than the illuminated area without resorting to step and repeat patterning. The step and repeat pattern transfer is not ideal when it is important to preserve detail in the junctions between fields. Excimer laser ablation was chosen for the manifold forming layer even though the level of detail in that part is relatively low. However, the inside edge of the manifold needed to be very sharp and to be precisely aligned (5 μm) to the back edge of the channel. The required sharpness and location accuracy was easily obtained by the excimer laser and would not be easily obtained by other fabrication methods.

9. RAPID PROTOTYPING AND LOW COST PRODUCTION

Laser micromaching of microfluidic structures can play an important role at all stages in the development of microfluidic devices. Different laser sources can cut a wide range of materials. Though we have concentrated on polymers for this presentation; metals, glass and ceramics can also be laser micromachined with accuracy and in many cases with speed. In rapid prototyping, galvanometer systems provide a high degree of flexibility in cutting any pattern through programmable motion. Image-wise transfer is effective with excimer lasers. Prototyping flexibility can be obtained by creative use of the mask to provide a wide range of building blocks that can be combined through programmable mask and substrate motions timed to laser firing. With the additional control of energy density and number of pulses on any area, wall shape and etch depth can be controlled. The high level of flexibility can permit rapid prototyping, rapid iteration, and incremental improvement in a microfluidic design. Thus, expensive and long lead die for die cutting, molds for injection molding, and presses for hot stamping can be avoided. Of course, these tools have an important place in the later stages of development and in production for some devices.

The ideal projects to undertake for micromachining are those where not only rapid prototyping in the early phases of a project are advantageous, but where laser micromachining also provides substantial production benefits. For patterning of adhesives and tapes where important feature sizes are <1 mm and where the tolerances are <0.1 mm, the galvanometer scanned CO_2 laser cutting appears to be highly advantaged in many cases. Of course, galvanometer scanned DPSS laser systems can be advantaged for patterning thin hard materials for microfluidics. The relatively low initial cost, low operating cost, and flexibility of galvo-scanned laser systems further enhance entry of these systems into production.

The effective use of excimer laser micromachining for production processes in microfluidics will usually require the confluence of several factors. Feature sizes <~50 μm, tight feature tolerances <~5 μm, densely packed features enabling use of an appreciable fraction of the laser light to do ablation, and fabrication in polymer substrates is one set of favorable factors. In some cases, photolithographic patterning of photoresists, polyimides, SU-8 are advantaged over excimer laser ablation. Other situations that could favor excimer laser micromachining are non-planar substrates, a requirement for non-photolithographic materials, multilayer assemblies, and 3-dimensional structures in a single substrate.

10.CONCLUSIONS

We have described a range of microfluidic structures and the integration of a number of these structures into inkjet printheads. Though these devices and the fabrication methods have been demonstrated for a particular application, the methods and concepts can be extended to a wide range of microfluidic applications. Laser micromachining can be important in both the concept development and in the production phases of the development of microfluidic devices.

ACKNOWLEDGEMENTS

The authors would like to acknowledge the support of William Greene, Rong Zhu, and John Adams in the building, maintaining, and operation of the laser micromachining lab. Assembly and packaging of many of the microfluidic devices was done by Almon Fisher and Peter John. Pascal Miller and Yin Hua Li at Resonetics, Inc., contributed hardware development and process development to the fluid seal work. Thanks also to our many colleagues who supported funding, contributed ideas, provided encouragement, and who did device testing.

REFERENCES

1. P. Cooley, D. Wallace, and B. Antohe, "Applications of ink-jet printing technology to bioMEMS and microfluidic systems," Proc. SPIE **4560**, p 177-187 (2001).

2. P. M. Martin, D. W. Matson, W. D. Bennett and D. J. Hammerstrom, "Fabrication of plastic microfluidic components," Proc. SPIE **3515**, p 172-176 (1998).

3. V. V. Kancharla, K. K. Hendrics, and S. Chen, "Micromachining of packaging materials for MEMS using lasers," Proc. SPIE **4557**, p 220-224 (2001).

4. E. C. Harvey and P. T. Rumsby, "Fabrication techniques and their application to produce novel micromachined structures and devices using excimer laser projection," Proc. SPIE **3223**, p 26-33 (1997).

5. M. Gower, "Excimer laser microfabrication and micromachining." Proc. SPIE **4088**, p 124-131 (2000).